

1 Warm temperature and mild water stress cooperatively promote root
2 elongation

3 Scott Hayes^{1*}, Cheuk Ka Leong¹, Wenyan Zhang¹, Marthe Lamain¹, Jasper Lamers¹, Thijs de Zeeuw¹,
4 Francel Verstappen¹, Andreas Hiltbrunner^{2,3} & Christa Testerink^{1*}

5 1. Laboratory of Plant Physiology, Wageningen University, Wageningen 6700 AA, The Netherlands

6 2. Institute of Biology II, Faculty of Biology, University of Freiburg, Freiburg, Germany

7 3. Signalling Research Centres BIOSS and CIBSS, University of Freiburg, Germany

8 ORCID:

9 SH 0000-0001-8943-6238

10 CKL 0000-0003-1994-2519

11 WZ 0000-0002-9746-4949

12 ML 0009-0001-2492-756X

13 JL 0000-0001-9807-5489

14 TZ 0000-0002-1758-0107

15 AH 0000-0003-0438-5297

16 CT 0000-0001-6738-115X

17
18 Email address for correspondence: Scott Hayes (scotanist@gmail.com) and Christa Testerink
19 (christa.testerink@wur.nl)

20 Summary

21 Warm temperatures have a dramatic effect on plant development. In shoots, stems elongate, and leaves
22 are raised in a developmental programme called thermomorphogenesis. This results in enhanced leaf
23 cooling capacity¹. Thermomorphogenesis is tightly intertwined with light signalling pathways. The level of
24 integration is so high that it has been proposed that shoot temperature sensing may have evolved from
25 the co-option of an existing light signalling pathway during the colonisation of land by plants². Roots also
26 undergo thermomorphogenesis, but the mechanism by which this occurs is less well understood. Main root
27 elongation is enhanced at warm temperatures, and this response is independent of many of the light and
28 temperature signalling components of the shoot³. Roots develop in darkness and so it is a reasonable
29 assumption that root temperature signalling is not through modulation of light signalling. It was recently
30 speculated that due to the close correlation between warm temperature and soil moisture content, root
31 temperature signalling could feasibly be related to water availability signals². In this study we tested the
32 interaction between temperature and water availability signalling in plant roots. We found that these
33 environmental factors co-operatively enhance main root elongation. This interaction effect was dependent
34 on SUCROSE NON-FERMENTING RELATED KINASE 2.2 (SnRK2.2) and SnRK2.3 and the E3 ubiquitin ligase
35 CONSTITUTIVELY PHOTOMORPHOGENIC 1 (COP1). We found that SnRK2.2 / 2.3 and COP1 have opposite
36 effects on the stability of the transcription factor ELONGATED HYPOCOTYL 5 (HY5) in elongation zone hair
37 cells. The stability of HY5 in these cell types generally corresponded to the degree of root elongation seen
38 in each mutant background. Our study reveals several molecular components of root
39 thermomorphogenesis and highlights the importance of an integrative approach to plant environmental
40 signalling. Our results may have direct implications for agricultural land management, especially as global
41 climates become more unpredictable.

42 Results and Discussion

43 To investigate the interaction between temperature and water availability on root growth, we grew
44 Arabidopsis seedlings on soil with a range of water contents, at either 20°C or 28°C. Water content was re-
45 established daily through watering the soil surface. We found when the soil water content was high (23%
46 to 19% water by weight- approx. 107% to 89% of field capacity), warm temperature did not induce root
47 elongation (Figure 1A). Only at soil water contents of 17% (approx. 79% field capacity) or lower did we
48 observe root thermomorphogenesis (Figure 1A). We noticed that these plants had a slight hypocotyl
49 phenotype. In well-watered soil, warm temperature strongly promoted hypocotyl elongation, as described
50 previously⁴. This effect tended to decrease somewhat in drier soils albeit not to a statistically significant

51 degree (Figure 1B). This effect is reminiscent of the recently reported inhibition of shade-induced hypocotyl
52 elongation under drought⁵. We compared the root and hypocotyl lengths of each plant in our assay and
53 found a weak negative correlation at 28°C, but not at 20°C (Figure S1A-B). This correlation did however
54 appear to be mostly a product of drought treatment groups, rather than any within treatment effect. SnRK2
55 kinases are well-established regulators of water stress signalling in plants⁶ and so we tested whether these
56 genes are required for the interaction between warm temperature and water stress on *Arabidopsis* seedling
57 architecture. We repeated our experiment at 21% and 17% soil water contents in the wild type and *snrk2.2*
58 / *snrk2.3* mutant. We found that wild type plants showed mild temperature-induced root elongation at
59 21% soil water content, but that the effect of temperature was greatly enhanced at 17% soil water content
60 (Figure 1C-D). The roots of a *snrk2.2* / *snrk2.3* mutant however behaved similarly to the wild type at 21%
61 soil water content and did not show a synergistic effect of warm temperature and water availability (Figure
62 1C-D). Warm temperature-induced hypocotyl elongation was slightly reduced by mild water stress in wild
63 type plants, but this was less pronounced in mutants lacking SnRK2.2 and SnRK2.3 (Figure 1E).

Figure 1

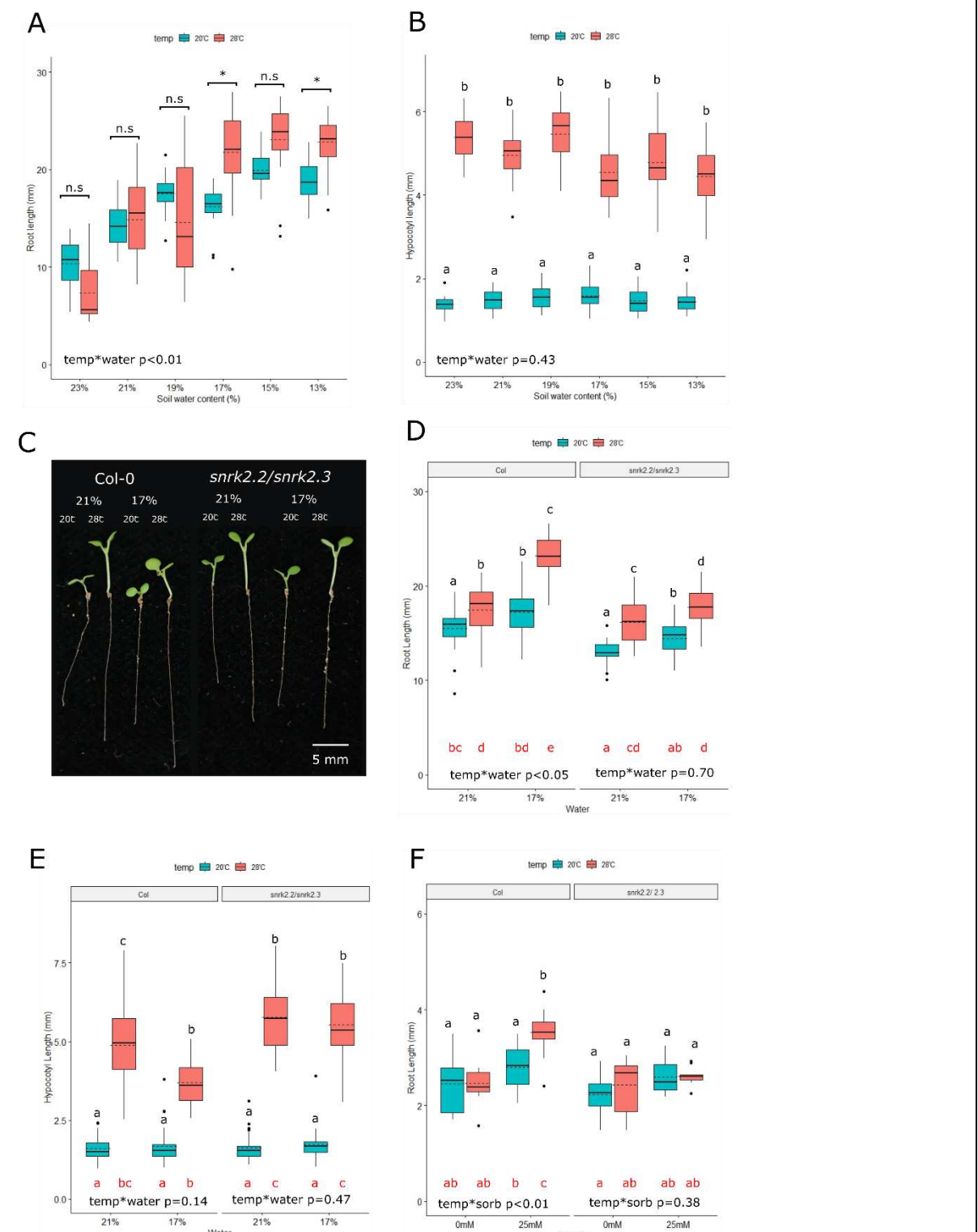


Figure 1. Warm temperature and mild water stress co-operatively promote root elongation. **A**) Root length of wild type (Col) arabidopsis plants grown on soil at different temperatures and water availabilities. Plants were sown directly onto soil of the indicated water content and germinated for 3 days under a propagator lid (150 μ E white light, 16h photoperiod, 20°C). Pots were then moved to 20°C or 28°C with the same lighting conditions for a further 4 days. Soil water content was re-established daily ($n \geq 19$). **B**) Hypocotyl lengths of the plants grown in A ($n \geq 19$). **C**) Representative images of Col and *snrk2.2 / snrk2.3* plants grown at 21% and 17% water as in A. **D**) Root lengths of plants grown as in C ($n=30$). **E**) Hypocotyl lengths of the plants grown in D ($n=30$). **F**) Root lengths of

Col and *snrk2.2* / *snrk2.3* seedlings that were germinated for 3 days in white light (150 μ E, 16h photoperiod, 20°C) on 1/10th MS media, before roots were detached and placed on 1/10th MS media supplemented with 5 mM sucrose and 0 mM or 25 mM sorbitol (n=14). Roots were grown in darkness for another 4 days at either 20°C or 28°C before measurement.

In each panel, *within genotype* interaction terms between environmental conditions are shown. In panels A, B, D and E, a Scheirer Ray Hare test and Dunn's post hoc test with a Benjamini-Hochberg correction were used. In panels F and G, a 2-way ANOVA with Tukey's HSD test was used. Black letters or asterisks indicate statistically significant means ($p < 0.05$) within each genotype. Red letters indicate statistically significant means ($p < 0.05$) across the whole experiment.

64

65 Roots can autonomously respond to warm temperature treatments³, but it has also been shown that there
66 is a genetic linkage between shoot and root thermomorphogenesis⁷. To investigate whether our root
67 phenotype was root autonomous, we adopted a detached root assay³. We first grew detached roots on
68 plates in the dark with a range of supplementary sucrose concentrations (Figure S1C). In the absence of
69 sucrose, we did not observe any root growth. At 5mM sucrose, we observed reasonable root elongation,
70 but not thermomorphogenesis. As sucrose concentrations increased however, roots gained the capacity to
71 respond to temperature. Sucrose acts as both an osmolyte and energy source. To investigate whether the
72 increase in osmotic stress was driving thermomorphogenesis, we grew detached roots on 5mM sucrose,
73 supplemented with a range of sorbitol concentrations (Figure S1D). We found that sorbitol also promoted
74 root thermomorphogenesis, and that this was dependent on SnRK2.2 and/ or SnRK2.3 (Figure 1F). We
75 were also able to induce the capacity for thermomorphogenesis in *Arabidopsis* by supplementing roots with
76 mannitol or sodium chloride at equimolar concentrations (Figure S1E). We observed a similar pattern of
77 responses in lettuce, leek, and radish roots, albeit with a weaker interaction term. This raises the possibility
78 that water availability and warm temperature cooperatively induce root elongation in a variety of
79 angiosperms (Figure S1F-H).

Figure S1

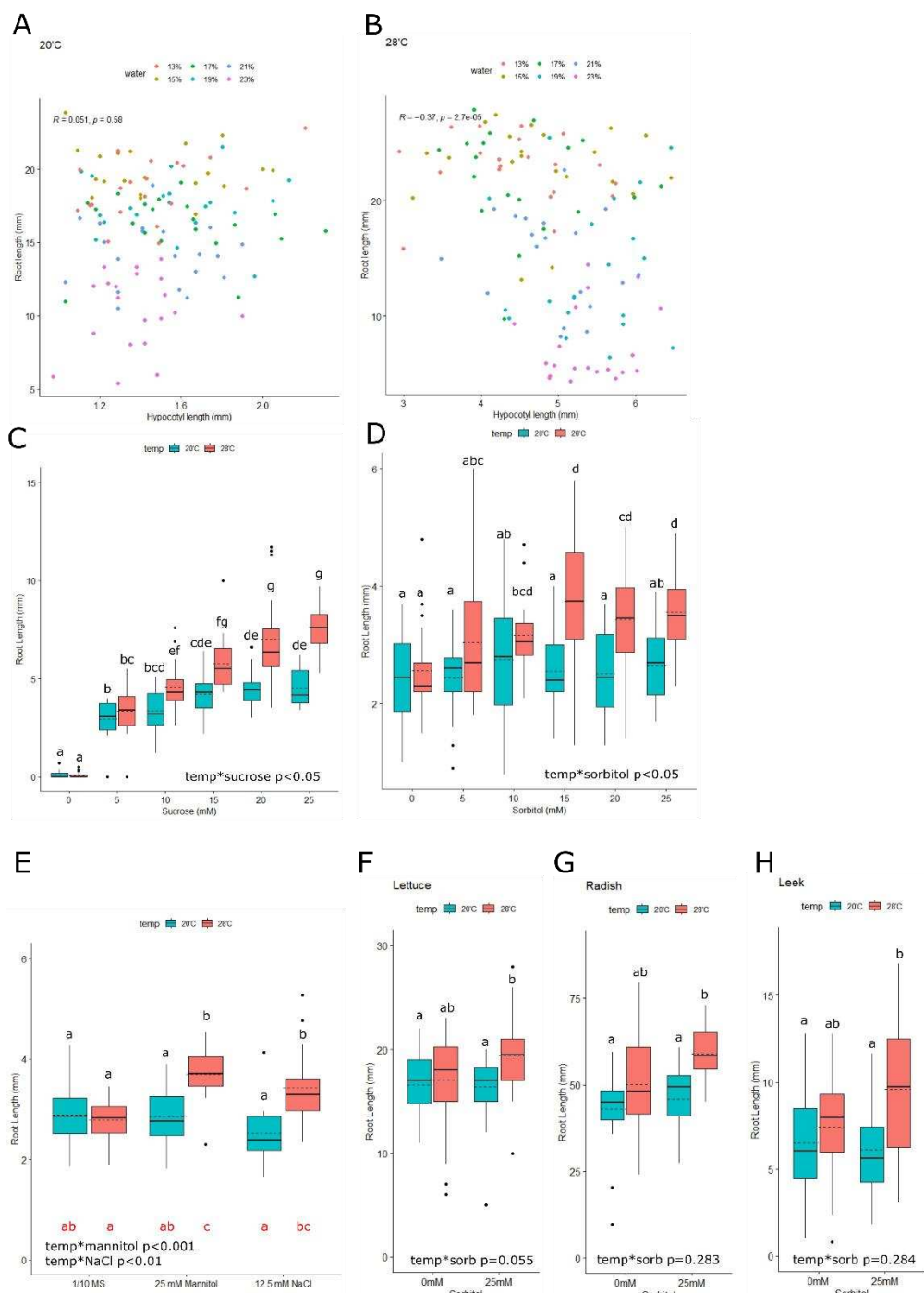


Figure S1. Warm temperature and mild water stress co-operatively promote root elongation. **A)** Correlation between root length and hypocotyl length of wild type (Col) *Arabidopsis* plants grown on soil at different water availabilities. Plants were sown directly onto soil of the indicated water content and germinated for 3 days under a propagator lid (150 μ E white light, 16h photoperiod, 20°C). Lids were removed, and pots were treated at 20°C with the same lighting conditions for a further 4 days. Soil water content was re-established daily ($n \geq 19$). **B)** Plants grown as in A, but for 4 days at 28°C after removal of the propagator lid. Note that panel S1A and S1B are a reanalysis of the data presented in Figure 1A and Figure 1B ($n \geq 19$). **C)** Root length of Col seedlings that were germinated for 3 days in white light (150 μ E, 16h photoperiod, 20°C) on 1/10th MS media, before roots were detached and placed on 1/10th MS media supplemented with various concentrations of sucrose. Roots were grown in darkness for another 4 days at either 20°C or 28°C before measurement ($n=24$). **D)** Root lengths of Col seedlings that were germinated for 3 days in white light (150 μ E, 16h photoperiod, 20°C) on 1/10th MS media, before roots were detached and placed on 1/10th MS media supplemented with 5mM sucrose and various concentrations of sorbitol. Roots were grown in darkness for another 4 days at either 20°C or 28°C before measurement ($n=24$). **E)** Root length of Col seedlings that were germinated for 3 days in white light (150 μ E, 16h photoperiod, 20°C) on 1/10th MS media, before roots were detached and placed on 1/10th MS media supplemented with various concentrations of mannitol or NaCl. Roots were grown in darkness for another 4 days at either 20°C or 28°C before measurement ($n=24$). **F)** Root length of Lettuce seedlings that were germinated for 3 days in white light (150 μ E, 16h photoperiod, 20°C) on 1/10th MS media, before roots were detached and placed on 1/10th MS media supplemented with 0 or 25mM sorbitol. Roots were grown in darkness for another 4 days at either 20°C or 28°C before measurement ($n=24$). **G)** Root length of Radish seedlings that were germinated for 3 days in white light (150 μ E, 16h photoperiod, 20°C) on 1/10th MS media, before roots were detached and placed on 1/10th MS media supplemented with 0 or 25mM sorbitol. Roots were grown in darkness for another 4 days at either 20°C or 28°C before measurement ($n=24$). **H)** Root length of Leek seedlings that were germinated for 3 days in white light (150 μ E, 16h photoperiod, 20°C) on 1/10th MS media, before roots were detached and placed on 1/10th MS media supplemented with 0 or 25mM sorbitol. Roots were grown in darkness for another 4 days at either 20°C or 28°C before measurement ($n=24$).

days at either 20°C or 28°C before measurement (n=24). **E**) Root lengths of lettuce seedlings that were germinated for 4 days in white light (150µE, 16h photoperiod, 20°C) on 1/10th MS media, before roots were detached and placed on 1/10th MS media supplemented with 5mM sucrose and 0 or 25mM sorbitol. Roots were grown in darkness for another 4 days at either 20°C or 28°C before measurement (n = 28). **F**) Root lengths of radish seedlings that were germinated for 4 days in white light (150µE, 16h photoperiod, 20°C) on 1/10th MS media, before roots were detached and placed on 1/10th MS media supplemented with 5mM sucrose and 0 or 25mM sorbitol. Roots were grown in darkness for another 3 days at either 20°C or 28°C before measurement (n ≥ 15). **G**) Root lengths of leek seedlings that were germinated for 7 days in white light (150µE, 16h photoperiod, 20°C) on 1/10th MS media, before roots were detached and placed on 1/10th MS media supplemented with 5mM sucrose and 0 or 25mM sorbitol. Roots were grown in darkness for another 3 days at either 20°C or 28°C before measurement (n ≥ 24). **H**) Root lengths of Col and *snrk2.2 / snrk2.3* seedlings that were germinated for 3 days in white light (150µE, 16h photoperiod, 20°C) on 1/10th MS media, before roots were detached and placed on 1/10th MS media supplemented with 5 mM sucrose and control, mannitol or NaCl (n=16). Roots were grown in darkness for another 4 days at either 20°C or 28°C before measurement.

In panels C-G, interaction terms between environmental conditions are shown. In panels A and B, Spearman's rank correlation coefficient was performed. In panels C and D, a Scheirer Ray Hare test and Dunn's post hoc test with a Benjamini-Hochberg correction were used. In panels F-G a 2-way ANOVA with Tukey's HSD test was used. Black letters or asterisks indicate statistically significant means (p< 0.05) within each genotype. Red letters indicate statistically significant means (p< 0.05) across the whole experiment.

80

81 SnRK2s are critical positive regulators of abscisic acid (ABA) signalling⁸. ABA is involved in a large number
82 of stress responses. We therefore tested whether ABA could also confer roots the capacity to elongate at
83 warm temperature. We found that low concentrations of ABA promoted root thermomorphogenesis, and
84 that this was also dependent on SnRK2 kinases (Figure 2A). Severe osmotic stress is known to promote
85 the accumulation of ABA⁸ and so we next tested whether ABA signalling was induced by mild osmotic stress
86 and warm temperature. To this end we utilised the *6xABRE-A:erGFP* reporter line, that contains six copies
87 of the abscisic acid response element from *ABA INSENSITIVE 1 (ABI1)*, driving the expression of an
88 endoplasmic reticulum localised GFP⁹. Surprisingly, we could not detect any effect of sorbitol on GFP
89 fluorescence in the root tip, instead we saw an increase in GFP signal at warm temperatures, particularly
90 in the QC and columella stem cells (Figure 2B, S2A-B). We were however unable to detect any changes in
91 ABA levels (in whole roots) across our experimental conditions (Figure 2C). We also observed an interaction
92 between osmotic stress and warm temperatures on root elongation in several mutants that are severely
93 deficient in ABA signalling (Figure 2D-E). We therefore propose that although ABA can mimic the effect of
94 osmotic stress on warm temperature-induced root elongation (Figure 1F and Figure 2A), it is not activation
95 of the canonical ABA signalling pathway *per se* that drives the combined response.

Figure 2

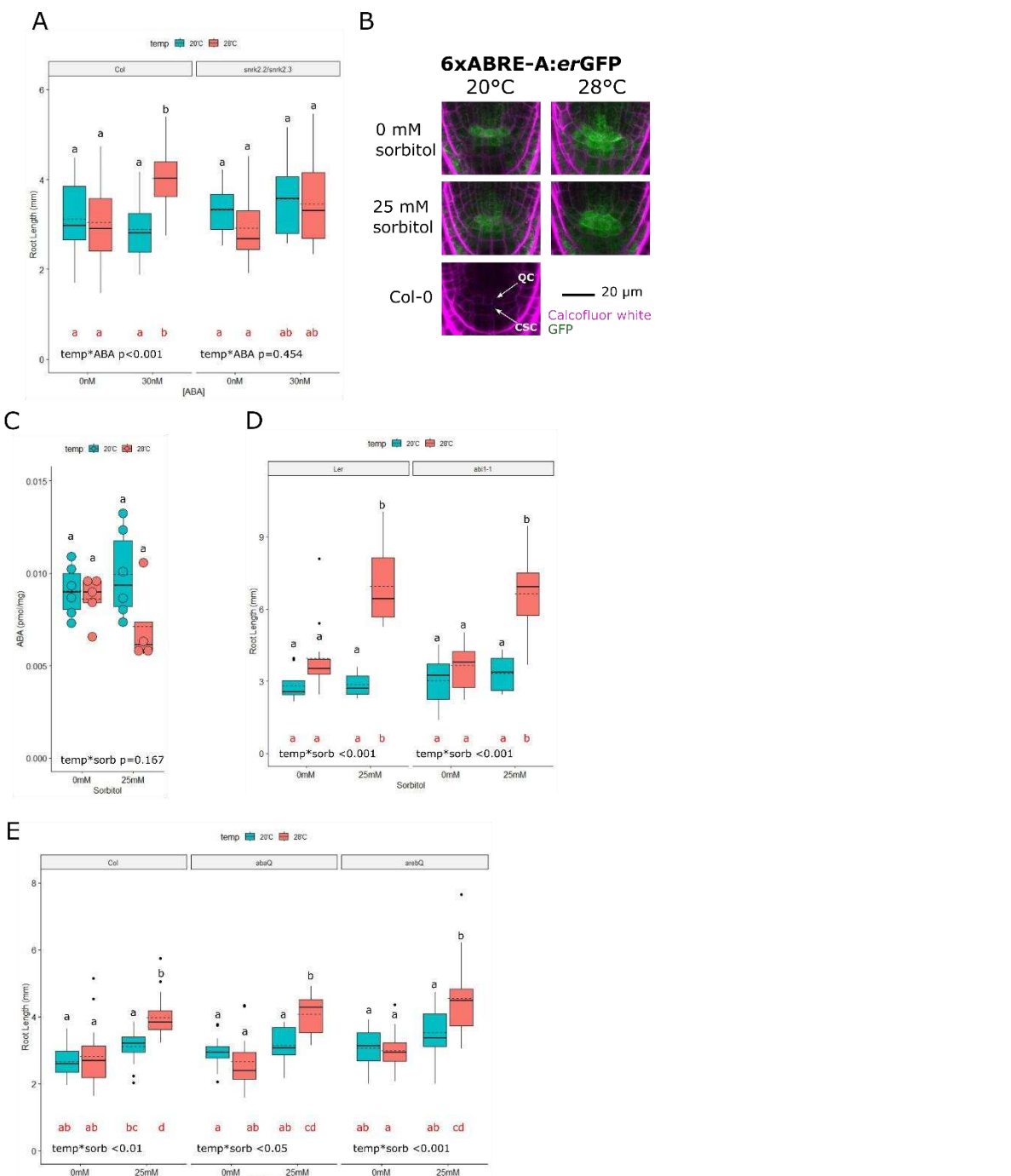


Figure 2. Warm temperature promotes ABA signalling in the root tip. **A)** Root lengths of Col and *snrk2.2 / snrk2.3* seedlings that were germinated for 3 days in white light (150 μ E, 16h photoperiod, 20 $^{\circ}$ C) on 1/10th MS media, before roots were detached and placed on 1/10th MS media supplemented with 5 mM sucrose and 0 nM or 30 nM ABA. Roots were grown in darkness for another 4 days at either 20 $^{\circ}$ C or 28 $^{\circ}$ C before measurement (n=16). **B)** Representative sum-stack images of the root tips of a 6xABRE-A:erGFP reporter line and Col wild type control. Plants were germinated for 3 days in white light (150 μ E, 16h photoperiod, 20 $^{\circ}$ C) on 1/10th MS media, before roots were detached and placed on 1/10th MS media supplemented with 5 mM sucrose and 0 mM or 25 mM sorbitol. Roots were grown in darkness for another 4 days at either 20 $^{\circ}$ C or 28 $^{\circ}$ C, before fixation. Quiescent centre (QC) and Columella stem cells (CSC) are indicated. **C)** ABA levels in the roots of wild type Col plants grown as in B (n \geq 4). **D)** Root lengths of wild type Ler and *abi1-1* plants grown as in B (n=12). **E)** Root lengths of

wild type Col, abaQ (*pyr1-1/pyl1-1/pyl2-1/pyl4-1*) and arebQ (*areb1/ areb2/ abf3/ abf1-1*) mutants grown as in B (n=16).

In each panel, *within genotype* interaction terms between environmental conditions are shown. A 2-way ANOVA with Tukey's HSD test was performed. Black letters indicate statistically significant means ($p < 0.05$) within each genotype. Red letters indicate statistically significant means ($p < 0.05$) across the whole experiment.

96

Figure S2

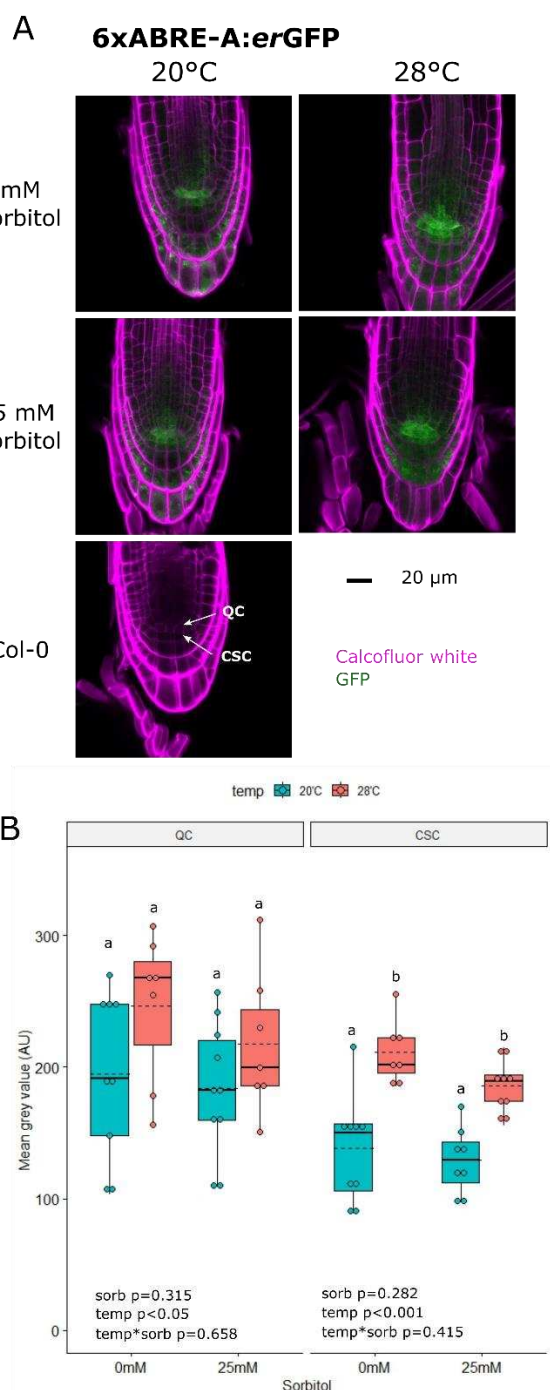


Figure S2. Warm temperature promotes ABA signalling in the root tip. **A)** Uncropped sum-stack images of the root tips shown in Figure 2B. Quiescent centre (QC) and Columella stem cells (CSC) are indicated. **B)** Quantification of GFP signal intensity from the QC and CSC of at least seven plants grown as in Figure 2B ($n \geq 7$). For each tissue type, a 2-way ANOVA with Tukey's HSD test was performed. Interaction terms between environmental conditions are shown. Different letters or asterisks indicate statistically significant means within each tissue.

Figure 3. COP1 suppresses warm temperature signalling in the absence of osmotic stress. Wild type Col, *cop1-4* and *cop1-6* mutant plants were germinated for 3 days in white light (150µE, 16h photoperiod, 20°C) on 1/10th MS media, before roots were detached and placed on 1/10th MS media supplemented with 5 mM sucrose and 0 mM or 25 mM sorbitol. Roots were grown in darkness for another 4 days at either 20°C or 28°C before being measured (n ≥ 8). **B)** Wild type Col plants were grown as in A but grown for the final 4 days in either darkness, 8 hours photoperiod (8h PP) or 16h PP white light (150µE) (n ≥ 13). **C)** Representative images of *pCOP1:mCherry-COP1* reporter lines grown as in A. Orthogonal sections were generated from the elongation zone. **D)** Root lengths of wild type Col, *cop1-4*, *snrk2.2/snrk2.3* and *cop1-4 / snrk2.2/ snrk2.3* lines grown as in A (n=16).

In each panel, *within genotype* interaction terms between environmental conditions are shown. In panels A and D, a 2-way ANOVA with Tukey's HSD test was performed. In panel B a Scheirer Ray Hare test and Dunn's post hoc test with a Benjamini-Hochberg correction was used. Black letters indicate statistically significant means (p< 0.05) within each genotype. Red letters indicate statistically significant means (p< 0.05) across the whole experiment.

97

98 In an effort to establish a molecular pathway for the control of mild osmotic stress and warm temperature-
99 induced root elongation, we tested mutants of genes that have established roles in shoot temperature-
100 signalling. The detached roots of plants deficient in *PIF1, 3, 4, 5* and *7* (*pifq/pif7-1*) behaved very similarly
101 to the wild type (Figure 3SA), confirming early reports that these genes are not required for local root
102 responses to warm temperature^{10,11}. We also found that the roots of mutants lacking phyA and phyB were
103 very similar to wild type roots (Figure S3B). *COP1* is essential for increased hypocotyl elongation at warm
104 temperature¹². We tested whether *COP1* plays a similar role in promoting root elongation. Surprisingly, we
105 found that the *cop1-4* mutant has very high root elongation at warm temperatures, both in the presence
106 and absence of osmotic stress (Figure 3A). The *cop1-6* mutant showed a similar trend, to a lower extent
107 (consistent with the weak phenotype of this mutant in the dark¹³). Light represses *COP1* activity¹⁴ and so
108 we tested the effect of light on our assay. Indeed, we found that light conferred roots with the ability to
109 respond to warm temperature, even in the absence of sorbitol (Figure 3B). We observed no additional
110 effect of light in *cop1-4* mutant (Figure 3SB). These results reveal *COP1* to be a repressor of warm
111 temperature / water stress signalling in roots. Most studies into warm temperature-induced root elongation
112 are performed in the light^{3,7,10,15,16}. This result could therefore explain why multiple groups have reported
113 warm temperature-induced elongation in the absence of water stress, and why warm temperature-
114 enhanced root elongation is reduced or lost in short photoperiod conditions^{15,16}.

Figure 3

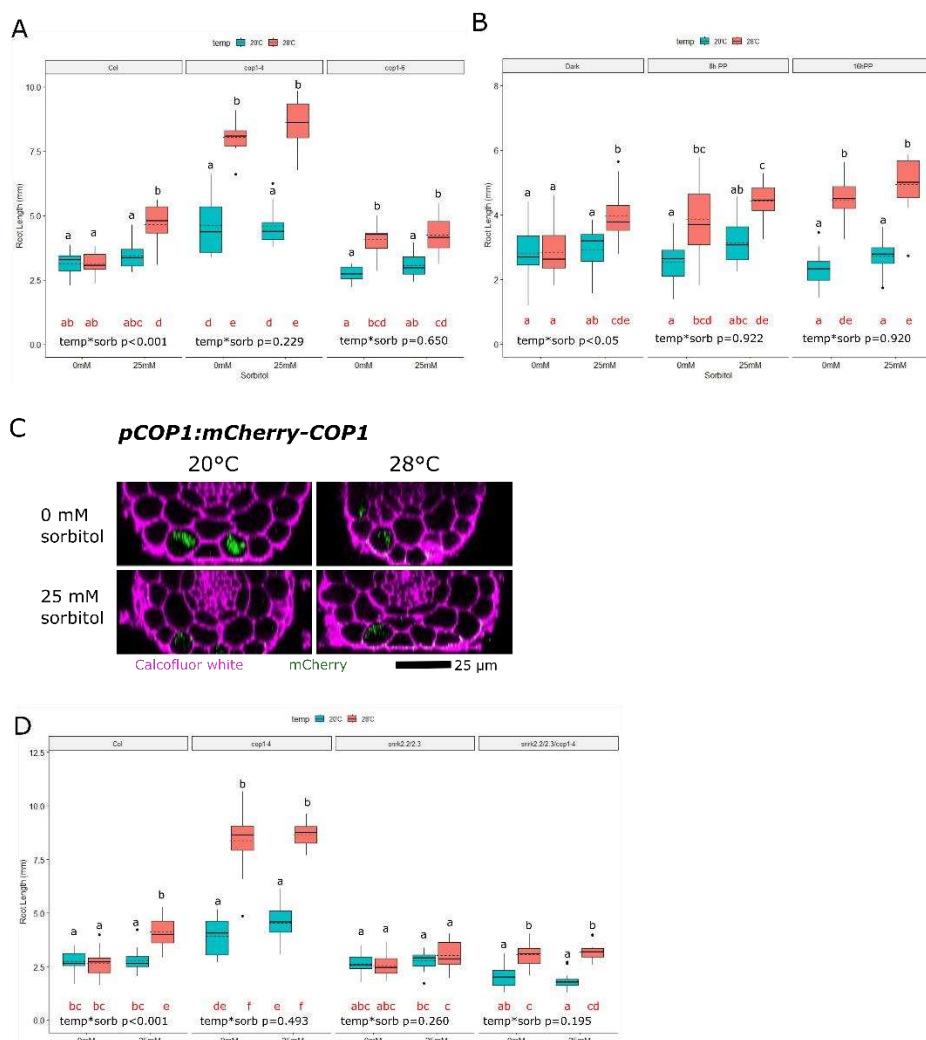


Figure 3. COP1 suppresses warm temperature signalling in the absence of osmotic stress. Wild type Col, *cop1-4* and *cop1-6* mutant plants were germinated for 3 days in white light (150μE, 16h photoperiod, 20°C) on 1/10th MS media, before roots were detached and placed on 1/10th MS media supplemented with 5 mM sucrose and 0 mM or 25 mM sorbitol. Roots were grown in darkness for another 4 days at either 20°C or 28°C before being measured (n ≥ 8). **B)** Wild type Col plants were grown as in A but grown for the final 4 days in either darkness, 8 hours photoperiod (8h PP) or 16h PP white light (150μE) (n ≥ 13). **C)** Representative images of *pCOP1:mCherry-COP1* reporter lines grown as in A. Orthogonal sections were generated from the elongation zone. **D)** Root lengths of wild type Col, *cop1-4*, *snrk2.2/snrk2.3* and *cop1-4 / snrk2.2 / snrk2.3* lines grown as in A (n=16). In each panel, *within genotype* interaction terms between environmental conditions are shown. In panels A and D, a 2-way ANOVA with Tukey's HSD test was performed. In panel B a Scheirer Ray Hare test and Dunn's post hoc test with a Benjamini-Hochberg correction was used. Black letters indicate statistically significant means (p < 0.05) within each genotype. Red letters indicate statistically significant means (p < 0.05) across the whole experiment.

115

116 We next questioned whether warm temperature or osmotic stress influenced COP1 abundance in the root.
 117 To this end, we produced a line expressing *mCherry-COP1* under its native promotor (*pCOP1:mCherry-COP1*). We were able to detect mCherry fluorescence in only a few specific cell types, namely the epidermal
 118 hair cells of the elongation zone and the endodermis of the differentiation zone and mature root (Figure
 119 S3C). When we grew these plants in our experimental conditions, we found that the mCherry signal in
 120 epidermal hair cells was highest at 20°C in the absence of sorbitol. Warm temperature and the presence
 121 of sorbitol both reduced the mCherry signal in this cell type (Figure 3C, S3D-E). This suggests that COP1
 122 abundance is reduced at either 28°C or in the presence of mild osmotic stress. Our initial hypothesis was
 123

124 that SnRK2s could contribute to root elongation in our experimental conditions through the suppression of
125 COP1. However, we did not see a reduction in mCherry-COP1 abundance upon the application of ABA
126 (Figure S3D-E). In fact, we saw that the application of ABA increased the abundance of mCherry-COP1 at
127 28°C. We also crossed our reporter into the *snrk2.2 / snrk2.3* background to see how this would affect
128 mCherry-COP1 abundance. We found that in the *snrk* mutant background, nuclear mCherry-COP1 was
129 barely detectable, lending support for the argument that the SnRKs are required to maintain COP1
130 abundance (Figure S3D-E). We found this result puzzling, as mutants with low COP1 abundance showed
131 enhanced warm temperature-induced root elongation even in the absence of sorbitol (Figure 2A). We
132 therefore tested the genetic interaction between COP1 and the SnRKs by generating *cop1-4/snrk2.2/2.3*
133 triple mutants. As previously, the *cop1-4* mutant elongated in response to temperature with and without
134 mild osmotic stress, and the *snrk2.2 / snrk2.3* mutant had lower root elongation than the wild type (Figure
135 3D). In the triple mutant however, we observed a similar pattern of root elongation as in the *cop1-4*
136 mutant, but with a greatly reduced amplitude (Figure 3D). This suggests that enhanced root elongation in
137 the absence of COP1 requires the presence of SnRKs. It also shows that warm temperature can promote
138 root elongation in the absence of SnRK2.2 / SnRK2.3 and COP1.

Figure S3

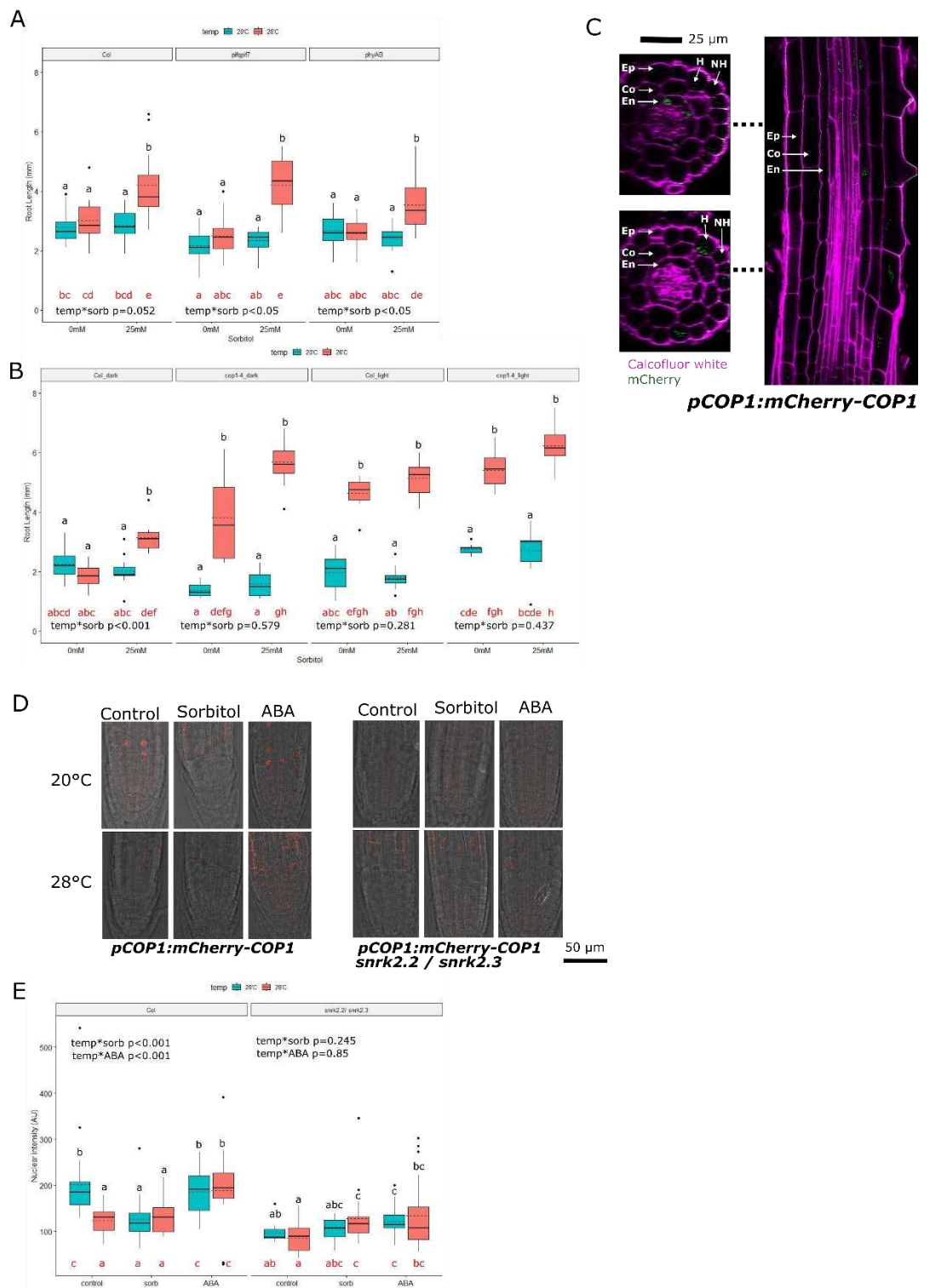


Figure S3. COP1 suppresses warm temperature signalling in the absence of osmotic stress. **A**) Wild type Col, *pif1-1 / pif3-3 / pif4-2 / pif5 / pif7-1* (*pifq / pif7*) and *phyA / phyB-9* (*phyAB*) mutant plants were germinated for 3 days in white light (150 μ E, 16h photoperiod, 20°C) on 1/10th MS media, before roots were detached and placed on 1/10th MS media supplemented with 5 mM sucrose and 0 mM or 25 mM sorbitol. Roots were grown in darkness for another 4 days at either 20°C or 28°C before being measured (n \geq 14). **B**) Wild type Col or *cop1-4* mutant plants were grown as in A, but after detachment, roots were grown for 4 days in either darkness or 150 μ E white light with a 16h photoperiod (n \geq 8). **C**) *pCOP1:mCherry-COP1* were grown for three days in white light (150 μ E, 16h photoperiod, 20°C) on 1/10th MS media, before roots were detached and placed on 1/10th MS media supplemented with 5 mM sucrose and 25 mM sorbitol. Roots were grown in darkness for another 4

days at 20°C before fixation. Virtual cross sections were made through the differentiation zone (upper) and the end of the elongation zone (lower). Epidermis (Ep), cortex (CO), and endodermis (En) are indicated. Within the epidermis, cells are also characterised as either hair (H) or non-hair (NH) cells depending on their number of contacts with cortex cells. **D**) Representative confocal microscopy images of *pCOP1:mCherry-COP1* roots in both the wild type and *snrk2.2 / snrk2.3* background. for three days in white light (150µE, 16h photoperiod, 20°C) on 1/10th MS media, before roots were detached and placed on 1/10th MS media supplemented with 5 mM sucrose and 25 mM sorbitol, 30 nM ABA or a negative control. Roots were grown in darkness for another 4 days at 20°C before fixation. Images show a 10µm sum stack projection, with red mCherry signal overlayed on a brightfield image in grey. **E**) Quantification of nuclear mCherry signal intensity of the three brightest nuclei from images of roots grown as in D (n ≥ 6 roots).

In each quantitative panel, *within genotype* interaction terms between environmental conditions are shown. In all panels, Scheirer Ray Hare test and Dunn's post hoc test with a Benjamini-Hochberg correction was used. Black letters indicate statistically significant means (p< 0.05) within each genotype / light condition. Red letters indicate statistically significant means (p< 0.05) across the whole experiment.

139

140 To gain more insight into the regulatory network controlling root elongation in mild osmotic stress and
141 warm temperature, we focused on identifying factors that could act downstream of COP1 and the SnRKs.
142 HY5 was recently identified as a key regulator of plant root thermomorphogenesis¹⁵. COP1 is known to
143 regulate HY5 abundance in response to warm temperature in the shoot¹² and so we tested whether this
144 regulatory module plays a role in the root. Indeed, we found that the exaggerated root elongation of the
145 *cop1-4* mutant was highly dependent on the presence of *HY5* (Figure 4A). HY5 has previously been shown
146 to be stabilised by warm temperature in the root¹⁵. We therefore tested how HY5 stability is regulated in
147 combined warm temperature and mild osmotic stress conditions, using a line expressing GFP-HY5 under a
148 constitutive promoter¹⁷. Because we observed COP1 in only a subset of epidermal cells in the elongation
149 zone (Figure 3C), we first investigated whether HY5 stability was differentially regulated in hair and non-
150 hair cells. We found that in non-hair cells (where mCherry-COP1 was not detected) warm temperature
151 promoted the stability of HY5 in both the presence and absence of sorbitol (Figure S4A-B). In hair cells by
152 contrast, we found that warm temperature reduces HY5 stability in absence of sorbitol but promotes HY5
153 stability in the presence of sorbitol (Figure S4A, Figure 4B-C). We crossed the HY5 reporter line into the
154 *cop1-4* background. We found that in the absence of COP1, hair cell localised HY5 is stabilised by warm
155 temperature in both presence and absence of sorbitol (Figure 4B-C). This pattern is similar to that of
156 root elongation in the *cop1-4* mutant (Figure 4A), suggesting that the misregulation of HY5 may be
157 responsible for enhanced root elongation in this mutant. We also crossed our GFP-HY5 reporter into the
158 *snrk2.2 / snrk2.3* background. We found that the stability of HY5 in hair cells was dramatically reduced in
159 the absence of SnRK2s (Figure 4B-C, Figure S4A). Interestingly though, despite its low abundance, the
160 pattern of HY5 regulation was comparable to the original reporter line. This suggests that SnRK2s are
161 important for maintaining HY5 abundance, but that warm temperature and mild osmotic stress are still
162 able to regulate HY5 abundance in the absence of SnRK2.2 and SnRK2.3.

Figure 4

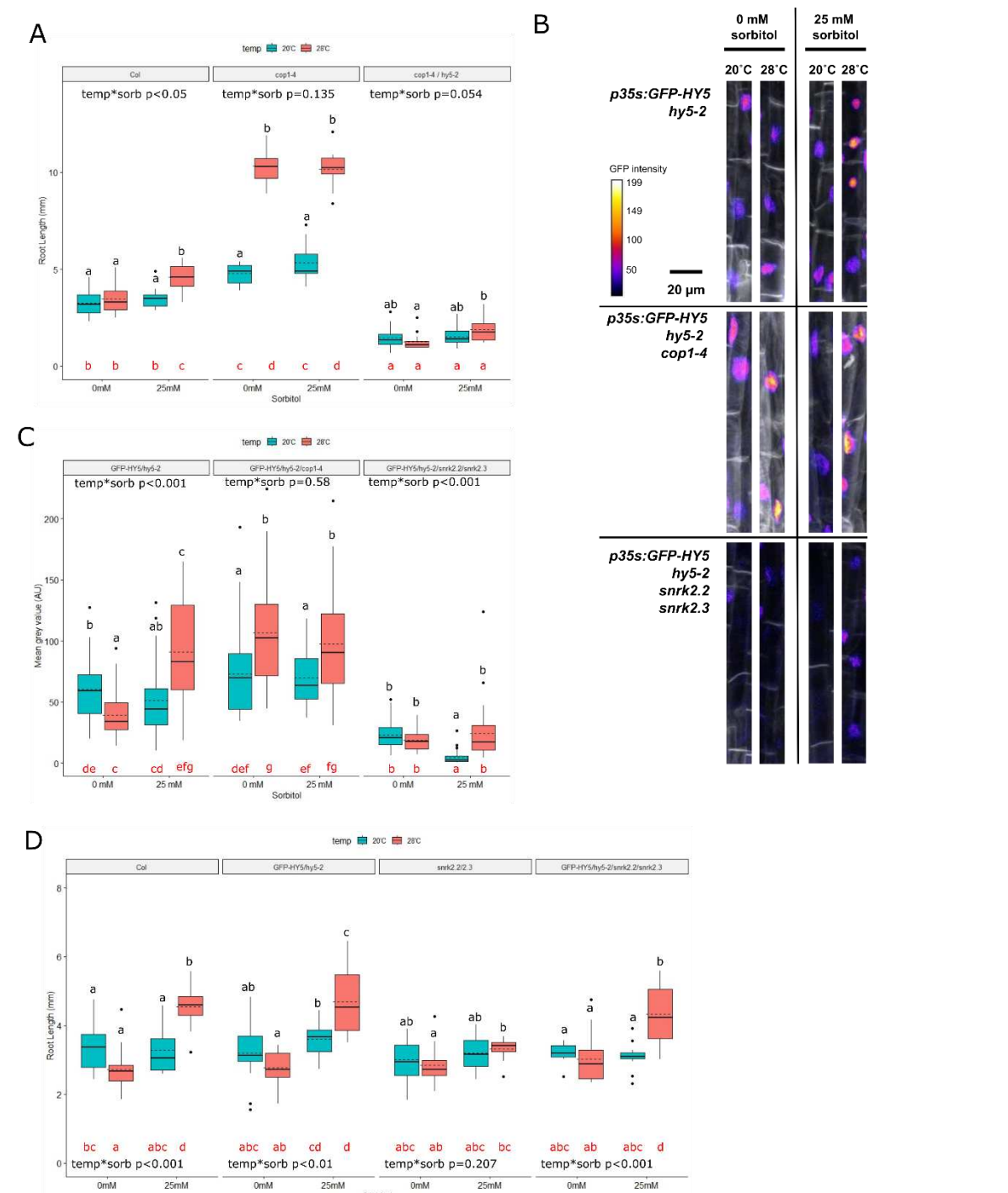


Figure 4: Warm temperature and mild water stress promote the accumulation of HY5. **A)** Root lengths of Col, *cop1* and *cop1* / *hy5-2* mutants grown for 3 days in white light (150 μ E, 16h photoperiod, 20°C) on 1/10th MS media, before roots were detached and placed on 1/10th MS media supplemented with 5 mM sucrose and 0 mM or 25 mM sorbitol. Roots were grown in darkness for another 4 days at either 20°C or 28°C before measurement (n=14). **B)** Sum slice image of the elongation zone hair cells of a *p35S:GFP-HY5* reporter in the *hy5*, *hy5/cop1* and *hy5 / snrk2.2 / snrk2.3* backgrounds. Seedlings were grown as in A before fixation. Calcofluor white stained cell walls are shown in grey. **C)** Mean grey value of hair cell nuclei from the images generated in B. Five nuclei were quantified from each root (n \geq 6 roots). **D)** Root lengths of Col, *p35S:GFP-HY5 / hy5-2*, *snrk2.2 / snrk2.3* and *p35S:GFP-HY5 / hy5-2 / snrk2.2 / snrk2.3* mutants grown as in A (n=14). In each panel, *within genotype* interaction terms between environmental conditions are shown. In panels A, a 2-way ANOVA with Tukey's HSD test was performed. In panels C and D, a Scheirer Ray Hare test and Dunn's post hoc test with a Benjamini-Hochberg correction was used. Black letters

indicate statistically significant means ($p < 0.05$) within each genotype. Red letters indicate statistically significant means ($p < 0.05$) across the whole experiment.

163

164 This finding prompted us to look at the root elongation phenotypes in our GFP-HY5 over-expressor lines.
165 We found that *GFP-HY5* / *hy5-2* had a similar phenotype to the wild type, with no temperature-induced
166 root elongation in the absence of sorbitol, but with temperature-induced root elongation in the presence
167 of sorbitol (Figure 4D). The *snrk2.2/snrk2.3* mutant behaved as previously, with no temperature-induced
168 root elongation in either the presence or absence of sorbitol. Interestingly though, the overexpression of
169 *GFP-HY5* in this mutant background was able to rescue the phenotype (Figure 4D). This suggests that
170 SnRK2.2 and SnRK2.3 may be a pre-requisite for basal HY5 stability in the root, but they are not *per se*
171 required for changes in HY5 abundance in response to warm temperature and mild osmotic stress.

172 Together, our findings lead us to propose a model whereby the stability of HY5 in hair cells of the elongation
173 zone is increased by warm temperature and mild osmotic stress. This stabilisation of HY5 correlates with
174 an increase in root elongation in these conditions. In the absence of mild osmotic stress, COP1 promotes
175 the degradation of HY5 specifically in these cells. In the presence of mild osmotic stress, COP1 abundance
176 is reduced, and this allows for the stabilisation of HY5. We propose that SnRK2.2 / SnRK2.3 are required
177 to maintain a background pool of HY5, and as such, warm temperature and osmotic stress no longer have
178 a combined effect on root elongation in the *snrk2.2/ snrk2.3* mutant (Figure S4C).

Figure S4

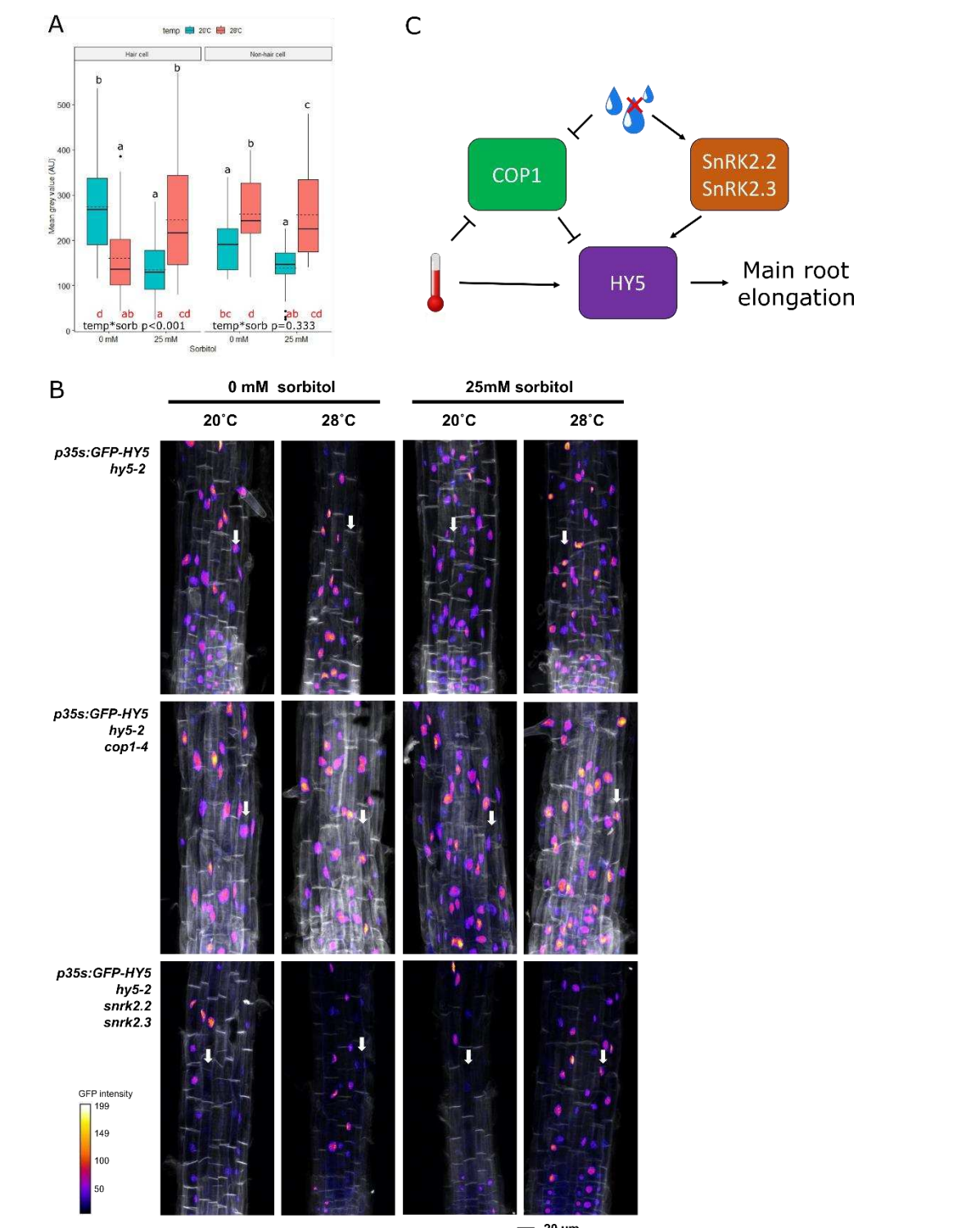


Figure S4: Warm temperature and mild water stress promote the accumulation of HY5. **A)** Mean grey value of hair and non-hair cell nuclei from sum stack images of *p35s:GFP-HY5* / *hy5-2* roots. Plants were grown for 3 days in white light (150 μ E, 16h photoperiod, 20°C) on 1/10th MS media, before roots were detached and placed on 1/10th MS media supplemented with 5 mM sucrose and 0 mM or 25 mM sorbitol. Roots were grown in darkness for another 4 days at either 20°C or 28°C before fixation. A Scheirer Ray Hare test and Dunn's post hoc test with a Benjamini-Hochberg correction was used to determine interactions between environmental conditions. Black letters indicate statistically significant means ($p < 0.05$) within each cell type. Red letters indicate statistically significant means ($p < 0.05$) across the whole experiment. At least three nuclei were quantified for each root ($n=6$ roots). **B)** Uncropped sum-stack images of the root tips shown in Figure 4B. Hair cell files are indicated with white arrows. **C)** A proposed working model for co-operative regulation of root elongation by water

stress and warm temperature. In the absence of water stress and at 20°C, COP1 suppresses HY5 in the elongation zone root hair cells. Under mild water stress at 20°C, COP1 abundance is reduced, but in the absence of warm temperature, this is not enough to promote HY5 stability. At 28°C, COP1 abundance is reduced, but this does not result in HY5 stabilisation if no water stress is present. In the presence of both warm temperatures and mild water stress, COP1 abundance is reduced, and HY5 stability is enhanced (possibly through the action of SnRKs).

179

180 The evidence presented in this manuscript paints a picture of a complex regulatory network that controls
181 root elongation in the presence of two commonly co-occurring stresses. It is possible that this network
182 operates as a negative feedback loop. HY5 directly promotes the expression of *COP1*¹⁸, and so our
183 unexpected finding of low *pCOP1:mCherry-COP1* abundance in the *snrk2.2 / snrk2.3* background (Figure
184 S3D-E) may be due to low HY5 stability in this line. We are not certain about how our data on the
185 *6xABRE_A:erGFP* reporter should be interpreted (Figure 2B). It is possible that this reporter is not reporting
186 on SnRK2 activity *per se*, but rather on HY5 activity in the whole meristem. The *6xABRE_A* reporter
187 contains multiple repeats of an ABA RESPONSIVE ELEMENT from the *ABI1* promoter⁹. HY5 also binds to
188 the promoter of this gene¹⁹ and so the activation of this reporter may reflect the general increase in HY5
189 stability seen at warm temperatures (Figure S4A-B).

190 Our study raises several important questions regarding the molecular basis for mild osmotic stress and
191 warm temperature signalling in the root. Firstly, what is the basis for HY5 stabilisation at warm
192 temperature? We have shown that COP1 and SnRK2.2/ SnRK2.3 gate this response, but we do not know
193 what factor actually promotes HY5 stability in these conditions. Plant shoots contain a multitude of
194 temperature sensors and so it is feasible that multiple points of temperature signal input also exist in roots.
195 Secondly, why do plant roots only elongate at warm temperature in the presence of osmotic stress? We
196 present genetic evidence for the role of COP1 in controlling this process (Figure 3A), but the reduction in
197 mCherry-COP1 accumulation at 28°C in the absence of sorbitol suggests additional signals are required to
198 activate HY5 in water stress conditions.

199 This study establishes that in plant roots, warm temperature and water stress signalling are intimately
200 entwined. This finding makes sense on a physiological level, as these environmental factors often occur in
201 combination²⁰. Importantly, although we approached this study from the point of view of temperature
202 signalling, our results can also be viewed from the opposite perspective. Warm temperature enhances the
203 response of roots to water stress. It may be that the increased water demands of the shoot at warm
204 temperature¹ necessitate that warm temperature and water stress signalling are tightly integrated in roots.
205 Our results provide a valuable starting point for further investigations into the combined control of root
206 elongation by warm temperature and mild osmotic stress. We hope that future research leads to further
207 elucidation of the molecular basis and physiological relevance of this response.

208

209 **Materials and Methods**

210 **KEY RESOURCES TABLE**

211 See Appendix 1

212 **CONTACT FOR REAGENT AND RESOURCE SHARING**

213 Further information and requests for resources and reagents should be directed to and will be fulfilled by
214 the Lead Contact, Christa Testerink

215 **EXPERIMENTAL MODEL AND SUBJECT DETAILS**

216 **Pre-existing lines**

217 The main experimental organism used in this study was *Arabidopsis thaliana*. Several mutant *Arabidopsis*
218 lines were described previously: *cop1-4*¹³, *cop1-6*¹³, *snrk2.2/snrk2.3*⁸, *6xABRE-A:erGFP*⁹, *abaQ*²¹, *arebQ*²²,
219 *cop1-4/hy5-2*²³, *pifq / pif7*²⁴, *phyAB*²⁵ and *p35s:GFP-HY5 / hy5-2*¹⁷ are in the Col-0 background. The *abi1-*

220 l^{26} mutant is in the Ler background. The original sources for these lines can be found in the Key Resources
221 Table.

222 In addition to Arabidopsis, lettuce (*Lactuca sativa* "Hilde II"), leek (*Allium porrum* "Herfstreuze 2") and
223 radish (*Raphanus sativus* "Saxa 2") were used.

224 **Lines developed in this study**

225 *pCOP1:mCherry-COP1*

226 A COP1 promoter fragment was PCR amplified from Col-0 genomic DNA using primers ah930/ah931,
227 digested with SpeI and SbfI, and ligated into *pPPO30A-phyA*²⁷ cut with AvrII/SbfI to replace the
228 *pPHYA:PHYA-YFP-terRbcS* cassette and resulting in plasmid *pPPO-pCOP1* (#3691). The RbcS terminator
229 was then cut from *pCHF70HA*²⁸ using XbaI/SbfI and ligated into *pPPO-pCOP1* (#3691) in the XbaI/SbfI
230 sites, resulting in *pPPO-pCOP1-BglII-XbaI-terRbcS* (#3694). Next, *myc-mCherry* CDS was PCR amplified
231 from *pCHF150myc*²⁸ (#2958) using primers ah933/ah934, digested with BamHI/XbaI, and ligated into
232 *pPPO-pCOP1-BglII-XbaI-terRbcS* (#3694) after cutting with BglII/XbaI. This resulted in plasmid *pPPO-*
233 *pCOP1-myc-mCherry-BglII-XbaI-RbcSter* (#3702). Finally, COP1 CDS was PCR amplified from
234 *pPPO70v1HA-COP1*²⁹ (#3100) using primers ah935/ah227, cut with BamHI/SpeI, and ligated into *pPPO-*
235 *pCOP1-myc-mCherry-BglII-XbaI-RbcSter* (#3702) after digestion with BglII/XbaI. This resulted in *pPPO-*
236 *pCOP1-myc-mCherry-COP1* (#3749). Plasmid #3749 *pPPO-pCOP1-myc-mCherry-COP1* was transformed
237 into Agrobacteria (*Rhizobium radiobacter*) by electroporation. Agrobacteria (C58) were then used for
238 transformation of Col-0 plants by floral dip³⁰. Transgenic lines were selected using 7.6 μ l I-1 Inspire
239 (Syngenta Agro AG, Dielsdorf, Switzerland)²⁷. Homozygous lines were confirmed by screening seedlings
240 for expression of myc-mCherry-COP1 using epifluorescence microscopy. A map of the final plasmid used
241 for transformation will be made available along with the raw data of this manuscript.

242 *pCOP1:mCherry-COP1 / snrk2.2 / snrk2.3*

243 This line was generated through crossing *pCOP1:mCherry-COP1* and *snrk2.2 / snrk2.3*. F2 Lines were
244 initially screened through their ability to germinate on 30 nM ABA plates. Homozygous lines were confirmed
245 by PCR.

246 *cop1-4/snrk2.2/snrk2.3*

247 This line was generated through crossing *cop1-4* and *snrk2.2 / snrk2.3*. F2 Lines were initially screened
248 through their ability to germinate on 30 nM ABA plates, and a *cop1* mutant phenotype in the dark.
249 Homozygous lines were confirmed by PCR.

250 *p35s:GFP-HY5 / hy5-2 / snrk2.2 / snrk2.3*

251 This line was generated through crossing *p35s:GFP-HY5 / hy5-2* and *snrk2.2 / snrk2.3*. F2 Lines were
252 initially screened through their ability to germinate on 30 nM ABA plates, and the detection of GFP signal
253 in the roots. Homozygous lines were confirmed by PCR.

254 *p35s:GFP-HY5 / hy5-2 / cop1-4*

255 This line was generated through crossing *p35s:GFP-HY5 / hy5-2* and *cop1-4*. F2 Lines were initially
256 screened through their *cop1* phenotype in the dark, and the detection of GFP signal in the roots.
257 Homozygous lines were confirmed by PCR.

258 **PLANT PROPAGATION**

259 To generate the Arabidopsis seed used in this study, plants were grown in rockwool substrate in
260 greenhouses at a 16-hour photoperiod and a temperature of 21°C. Nutrients were supplied throughout the
261 growth cycle through Hyponex solution (pH5.8). Plants were kept well-watered until siliques senesced,
262 after which water was increasingly withheld until the plant was fully senesced. Harvested seeds were stored
263 dry at room temperature for at least 2 weeks before use.

264 **METHOD DETAILS**

265 **Root and Hypocotyl Length assay**

266 For physiological assays of *Arabidopsis* plants conducted in soil, seeds were sown directly onto 1kg of soil
267 at either 13%, 15%, 17%, 19%, 21% or 23% water content. Seeds were then germinated for 3 days
268 under a propagator lid (150μE white light, 16h photoperiod, 20°C). No noticeable difference in germination
269 time was observed in these conditions. At day 3, propagator lids were removed, and pots were then placed
270 at either 20°C or 28°C with the same lighting conditions for a further 4 days. Soil water content was re-
271 established daily by dripping water onto the soil surface to a weight of 1kg. On day 7, seedlings were
272 excavated. This was achieved through gently holding them under the cotyledons, whilst water was sprayed
273 to excavate the root. Seedlings were then laid onto agar plates and scanned.

274 For physiological assay of *Arabidopsis* plants conducted on agar plates, seeds were surface-sterilised and
275 then sowed on 1/10th Murashige and Skoog medium including vitamins (Duchefa Biochemie),
276 supplemented with 0.5 g/ l MES (Duchefa Biochemie) and 0.8% Diashin Agar (Duchefa Biochemie), pH5.8.
277 After 3-4 days of stratification in dark at 4°C, plates with seed were then placed vertically at 90° in a
278 growth chamber for 3 days in white light (100μE, 16h photoperiod, 20°C) to stimulate germination. At day
279 3, roots were detached and placed on the same media, supplemented with 5 mM sucrose (Duchefa
280 Biochemie) unless otherwise stated. For osmotic stress and ABA treatments, the medium was additionally
281 supplemented with 25 mM sorbitol (Duchefa Biochemie), 25 mM mannitol (Duchefa Biochemie), 12.5 mM
282 NaCl (Duchefa Biochemie) or 30 nM ABA (Duchefa Biochemie) unless otherwise stated. Root tip position
283 was marked after detachment, and roots were grown in darkness for another 4 days at either 20°C or
284 28°C before being measured.

285 For physiological assay of lettuce and radish and leek, plants were grown as stated above for *Arabidopsis*,
286 but with an altered timetable. Lettuce and radish were germinated for 4 days in white light, and detached
287 roots were grown for another 4 days with or without sorbitol, and at either 20°C or 28°C. Leek seeds
288 were germinated for 7 days at the same conditions, and detached roots were grown for a further 4 days
289 before plates were scanned.

290 **Abscisic acid level measurements**

291 Wild type *Arabidopsis* (Col-0) were grown on plates similarly to as above for root lengths assays. One
292 minor modification was that seeds were germinated on plates covered with sterile mesh strips to facilitate
293 the dissection. 60 roots (approximately 5 mg) per sample were harvested in 2ml Eppendorf tubes
294 containing two 1/8" steel ball bearings (Weldtite, 3906141) and flash frozen in liquid nitrogen. Extraction
295 and purification was performed as previously described ³¹, with minor modifications. Samples were ground
296 2 x 30s at 25 rev/s. Stable isotope-labeled internal standards (100 nM in 10% methanol) were added to
297 ground samples (see Supplementary Table S2). Solvents were removed with a speed vacuum system
298 (thermoSavant) and a StrataX 30mg/3ml spe-column (Phenomenex) was used for purification.

299 ABA detection and quantification was done using liquid chromatography-tandem mass spectroscopy ³².
300 Sample residues were dissolved in 100μL acetonitrile /water (20:80 v/v) and filtered through a 0.2 μm
301 nylon centrifuge spin filter (BGB Analytik). Retention time was assessed using a Waters XevoTQS mass
302 spectrometer equipped with an electrospray ionization source coupled to an Acquity UPLC system (Waters).
303 Acetonitrile/water (+ 0.1 % formic acid) on a Acquity UPLC BEH C18 column (2.1 mm x100 mm, 1.7μm,
304 Waters) at 40 °C with a flowrate of 0.25 mL/min was used to perform chromatographic separations. The
305 column was equilibrated for 30 minutes with the solvent (acetonitrile /water (20:80 v/v) + 0.1% formic
306 acid). 5 μL of sample was injected for analysis, followed by an elution program where the acetonitrile
307 fraction linearly increased from 20% (v/v) to 70% (v/v) in 17 minutes. The acetonitrile fraction was
308 increased between samples to 100% and maintained there for one minute to wash the column. The
309 acetonitrile fraction was set to 20 % before injecting the next sample in one minute and maintained at this
310 concentration for one minute. A capillary voltage of 2.5 kV was combined with a source temperature of
311 150 °C and desolvation temperature of 500 °C. Quantification was done using multiple reaction monitoring.
312 MRM-setting optimization for the different compounds was done using the IntelliStart MS Console

313 (Supplementary Table S2). Peaks were analyzed using Targetlynx software and samples were normalized
314 for the internal standard recovery (ABA) and expressed relative to the sample fresh weight. Concentration
315 (pmol/mg fresh weight) was determined using a standard curve.

316 **Confocal imaging**

317 All roots were fixed in 4% paraformaldehyde (Sigma) dissolved in phosphate-buffered saline (PBS, Merck)
318 for 30 minutes under a vacuum, before washing twice in PBS. In some cases, tissues were cleared using
319 ClearSee³³ (10% w/v xylitol (Sigma), 15% w/v sodium deoxycholate (Sigma), 25% w/v urea (Sigma) for
320 between 1 day and three weeks depending on the experiment. Cell walls were stained with 0.05%
321 Calcofluor white (Megazyme) in ClearSee for 30min and then destained in ClearSee for 30min. Images
322 were collected using a Leica TCS SP8 HyD confocal microscope. For Calcofluor white, an excitation laser of
323 405 nm and a 425 nm to 475nm band-pass filter was used. For mCherry, an excitation laser of 552 nm
324 and a 590 nm to 630 nm band-pass filter was used. For GFP, an excitation laser of 448 nm and 500 nm to
325 550 nm band-pass filter was used. Images were acquired using a HC PL APO CS2 63x NA1.40 oil immersion
326 or a 40x water immersion objective fitted with a HyD detector. Within experiments, pinhole, gain, laser
327 power, mode of detection, dynamic range and detector offset were kept constant. Orthogonal sections
328 were re-constructed from z-stack images within the Leica Las-X imaging software.

329 **QUANTIFICATION AND STATISTICAL ANALYSES**

330 **Image quantification**

331 For root length data, plates were scanned on a flatbed scanner. Scans was quantified in ImageJ, using the
332 freehand line tool.

333 For fluorescence intensity measurements, confocal images in .lif format were opened in ImageJ. In figure
334 2, sum stack Z-projections were made, and the region of interest (either the QC or CSC) was highlighted
335 and mean grey value collected. In figure 4, nuclei were first isolated by thresholding before selection and
336 quantification.

337 **Data presentation**

338 Individual figures were made in R, using the "ggpubr" package. Final figures were collated in Inkscape.

339 **Statistical analyses**

340 Statistical tests were performed in R. Each figure in the manuscript represents a single experiment. Each
341 experiment was performed at least twice with similar results. For each individual experiment, a Levene
342 test ("car" package) was performed to test for homogeneity of the residuals. For datasets that had equal
343 variance, a 2-way ANOVA ("stats" and "multcompView" packages) was performed. For datasets in which
344 the variance was not homogenous, a Scheirer Ray Hare test ("rcompanion" and "FSA" packages) was
345 performed.

346 **ACKNOWLEDGEMENTS**

347 Work in Wageningen was supported by grants from European Research Council (ERC) under the European
348 Union's Horizon 2020 research and innovation programme (grant agreement no. 724321; ERC Consolidator
349 Grant Sense2SurviveSalt- CT), The Dutch Research Council (NWO) (Vici grant; VI.C.192.033- CT) and the
350 Wageningen Graduate School Postdoc Talent Programme (2019- SH).

351 Work in Freiburg was supported by the German Research Foundation (DFG) under Germany's Excellence
352 Strategy (EXC-2189 – Project ID 390939984- AH).

353 We would like to thank Ronald Pierik (Wageningen University) for supplying the *snrk2.2/2.3* line, Salomé
354 Prat (CRAG, Barcelona) for the *cop1-4*, *cop1-6*, *pifqif7*, *abaQ*, *arebQ* and *phyAB* lines, Charlotte Gommers
355 (Wageningen University) for the *cop1-4* / *hy5-215* line, José Dinneny (Stanford University) for the
356 *6xABRE-A:erGFP* line and Sang Yeol Lee (Gyeongsang National University) for the *p35S:GFP-HY5* / *hy5-2*
357 line. This work would not have been possible without your generosity.

358 **DATA AVAILABILITY**

359 All raw data and the code used to analyse and present this data will be posted at an online repository upon
360 publication of this manuscript. For access to biological stocks, please get in touch with the Lead Contact,
361 Christa Testerink at christa.testerink@wur.nl.

362 **References**

- 363 1. Crawford, A.J., McLachlan, D.H., Hetherington, A.M., and Franklin, K.A. (2012). High temperature
364 exposure increases plant cooling capacity. *Current Biology* 22, R396–R397.
365 10.1016/J.CUB.2012.03.044.
- 366 2. Ludwig, W., Hayes, S., Trenner, J., Delker, C., and Quint, M. (2021). On the evolution of plant
367 thermomorphogenesis. *J Exp Bot* 72, 7345–7358. 10.1093/JXB/ERAB310.
- 368 3. Bellstaedt, J., Trenner, J., Lippmann, R., Poeschl, Y., Zhang, X., Friml, J., Quint, M., and Delkera,
369 C. (2019). A Mobile Auxin Signal Connects Temperature Sensing in Cotyledons with Growth
370 Responses in Hypocotyls. *Plant Physiol* 180, 757–766. 10.1104/PP.18.01377.
- 371 4. Hayes, S., Sharma, A., Fraser, D.P., Trevisan, M., Cragg-Barber, C.K., Tavridou, E., Fankhauser,
372 C., Jenkins, G.I., and Franklin, K.A. (2017). UV-B Perceived by the UVR8 Photoreceptor Inhibits
373 Plant Thermomorphogenesis. *Current Biology* 27. 10.1016/j.cub.2016.11.004.
- 374 5. Semmoloni, M., Rojas, C.C., Yan, Y., Cao, X., and Casal, J.J. (2022). Water shortage reduces
375 PHYTOCHROME INTERACTING FACTOR 4, 5 and 3 expression and shade avoidance in *Arabidopsis*.
376 bioRxiv, 2022.12.02.518848. 10.1101/2022.12.02.518848.
- 377 6. Fujita, Y., Nakashima, K., Yoshida, T., Katagiri, T., Kidokoro, S., Kanamori, N., Umezawa, T.,
378 Fujita, M., Maruyama, K., Ishiyama, K., et al. (2009). Three SnRK2 protein kinases are the main
379 positive regulators of abscisic acid signaling in response to water stress in *arabidopsis*. *Plant Cell Physiol* 50. 10.1093/pcp/pcp147.
- 381 7. Gaillochet, C., Burko, Y., Platret, M.P., Zhang, L., Simura, J., Willige, B.C., Kumar, S.V., Ljung, K.,
382 Chory, J., and Busch, W. (2020). HY5 and phytochrome activity modulate shoot-to-root
383 coordination during thermomorphogenesis in *Arabidopsis*. *Development (Cambridge)* 147.
384 10.1242/dev.192625.
- 385 8. Fujii, H., Verslues, P.E., and Zhu, J.K. (2007). Identification of Two Protein Kinases Required for
386 Abscisic Acid Regulation of Seed Germination, Root Growth, and Gene Expression in *Arabidopsis*.
387 *Plant Cell* 19, 485–494. 10.1105/TPC.106.048538.
- 388 9. Wu, R., Duan, L., Pruneda-Paz, J.L., Oh, D.H., Pound, M., Kay, S., and Dinneny, J.R. (2018). The
389 6xABRE Synthetic Promoter Enables the Spatiotemporal Analysis of ABA-Mediated Transcriptional
390 Regulation. *Plant Physiol* 177, 1650–1665. 10.1104/PP.18.00401.
- 391 10. Ai, H., Bellstaedt, J., Bartusch, K.S., Eschen-Lippold, L., Babben, S., Balcke, G.U., Tissier, A.,
392 Hause, B., Andersen, T.G., Delker, C., et al. (2023). Auxin-dependent regulation of cell division
393 rates governs root thermomorphogenesis. *EMBO J* 42. 10.15252/embj.2022111926.
- 394 11. Borniego, M.B., Costigliolo-Rojas, C., and Casal, J.J. (2022). Shoot thermosensors do not fulfil the
395 same function in the root. *New Phytologist*. 10.1111/NPH.18332.
- 396 12. Park, Y.J., Lee, H.J., Ha, J.H., Kim, J.Y., and Park, C.M. (2017). COP1 conveys warm temperature
397 information to hypocotyl thermomorphogenesis. *New Phytologist* 215, 269–280.
398 10.1111/NPH.14581.
- 399 13. McNells, T.W., Von Arnim, A.G., Araki, T., Komeda, Y., Miséra, S., and Deng, X.W. (1994).
400 Genetic and molecular analysis of an allelic series of *cop1* mutants suggests functional roles for
401 the multiple protein domains. *Plant Cell* 6. 10.2307/3869929.

- 402 14. McNellis, T.W., Von Arnim, A.G., and Deng, X.W. (1994). Overexpression of arabidopsis COP1
403 results in partial suppression of light-mediated development: Evidence for a light-inactivable
404 repressor of photomorphogenesis. *Plant Cell* 6. 10.2307/3869976.
- 405 15. Lee, S., Wang, W., and Huq, E. (2021). Spatial regulation of thermomorphogenesis by HY5 and
406 PIF4 in Arabidopsis. *Nature Communications* 2021 12:1 12, 1–12. 10.1038/s41467-021-24018-7.
- 407 16. Martins, S., Montiel-Jorda, A., Cayrel, A., Huguet, S., Roux, C.P. Le, Ljung, K., and Vert, G.
408 (2017). Brassinosteroid signaling-dependent root responses to prolonged elevated ambient
409 temperature. *Nature Communications* 2017 8:1 8, 1–11. 10.1038/s41467-017-00355-4.
- 410 17. Nawkar, G.M., Kang, C.H., Maibam, P., Park, J.H., Jung, Y.J., Chae, H.B., Chi, Y.H., Jung, I.J.,
411 Kim, W.Y., Yun, D.J., et al. (2017). HY5, a positive regulator of light signaling, negatively controls
412 the unfolded protein response in Arabidopsis. *Proc Natl Acad Sci U S A* 114.
413 10.1073/pnas.1609844114.
- 414 18. Huang, X., Ouyang, X., Yang, P., Lau, O.S., Li, G., Li, J., Chen, H., and Deng, X.W. (2012).
415 Arabidopsis FHY3 and HY5 Positively Mediate Induction of COP1 Transcription in Response to
416 Photomorphogenic UV-B Light. *Plant Cell* 24, 4590. 10.1105/TPC.112.103994.
- 417 19. Burko, Y., Seluzicki, A., Zander, M., Pedmale, U. V., Ecker, J.R., and Chory, J. (2020). Chimeric
418 activators and repressors define HY5 activity and reveal a light-regulated feedback mechanism.
419 *Plant Cell* 32. 10.1105/tpc.19.00772.
- 420 20. Livneh, B., and Hoerling, M.P. (2016). The physics of drought in the U.S. Central Great Plains. *J
421 Clim* 29. 10.1175/JCLI-D-15-0697.1.
- 422 21. Park, S.Y., Fung, P., Nishimura, N., Jensen, D.R., Fujii, H., Zhao, Y., Lumba, S., Santiago, J.,
423 Rodrigues, A., Chow, T.F.F., et al. (2009). Abscisic acid inhibits type 2C protein phosphatases via
424 the PYR/PYL family of START proteins. *Science* (1979) 324. 10.1126/science.1173041.
- 425 22. Yoshida, T., Fujita, Y., Maruyama, K., Mogami, J., Todaka, D., Shinozaki, K., and Yamaguchi-
426 Shinozaki, K. (2015). Four Arabidopsis AREB/ABF transcription factors function predominantly in
427 gene expression downstream of SnRK2 kinases in abscisic acid signalling in response to osmotic
428 stress. *Plant Cell Environ* 38. 10.1111/pce.12351.
- 429 23. Oyama, T., Shimura, Y., and Okada, K. (1997). The Arabidopsis HY5 gene encodes a bZIP protein
430 that regulates stimulus-induced development of root and hypocotyl. *Genes Dev* 11, 2983–2995.
431 10.1101/GAD.11.22.2983.
- 432 24. Zhang, Y., Pfeiffer, A., Tepperman, J.M., Dalton-Roesler, J., Leivar, P., Grandio, E.G., and Quail,
433 P.H. (2020). Central clock components modulate plant shade avoidance by directly repressing
434 transcriptional activation activity of PIF proteins. *Proc Natl Acad Sci U S A* 117.
435 10.1073/pnas.1918317117.
- 436 25. Xing Liang Liu, Covington, M.F., Fankhauser, C., Chory, J., and Wagner, D.R. (2001). ELF3
437 encodes a circadian clock-regulated nuclear protein that functions in an Arabidopsis PHYB signal
438 transduction pathway. *Plant Cell* 13. 10.1105/tpc.13.6.1293.
- 439 26. Bertauche, N., Leung, J., and Giraudat, J. (1996). Protein phosphatase activity of abscisic acid
440 insensitive 1 (ABI1) protein from *Arabidopsis thaliana*. *Eur J Biochem* 241. 10.1111/j.1432-
441 1033.1996.0193t.x.
- 442 27. Rausenberger, J., Tscheuschler, A., Nordmeier, W., Wüst, F., Timmer, J., Schäfer, E., Fleck, C.,
443 and Hiltbrunner, A. (2011). Photoconversion and nuclear trafficking cycles determine
444 phytochrome A's response profile to far-red light. *Cell* 146. 10.1016/j.cell.2011.07.023.
- 445 28. Enderle, B., Sheerin, D.J., Paik, I., Kathare, P.K., Schwenk, P., Klose, C., Ulbrich, M.H., Huq, E.,
446 and Hiltbrunner, A. (2017). PCH1 and PCHL promote photomorphogenesis in plants by controlling

- 447 phytochrome B dark reversion. *Nature Communications* 2017 8:1 8, 1–9. 10.1038/S41467-017-
448 02311-8.
- 449 29. Sheerin, D.J., Menon, C., Oven-Krockhaus, S. Zur, Enderle, B., Zhu, L., Johnen, P.,
450 Schleifenbaum, F., Stierhof, Y.D., Huq, E., and Hiltbrunner, A. (2015). Light-activated
451 phytochrome A and B interact with members of the SPA family to promote photomorphogenesis
452 in arabidopsis by reorganizing the COP1/SPA complex. *Plant Cell* 27. 10.1105/tpc.114.134775.
- 453 30. Clough, S.J., and Bent, A.F. (1998). Floral dip: A simplified method for Agrobacterium-mediated
454 transformation of *Arabidopsis thaliana*. *Plant Journal* 16. 10.1046/j.1365-313X.1998.00343.x.
- 455 31. Floková, K., Tarkowská, D., Miersch, O., Strnad, M., Wasternack, C., and Novák, O. (2014).
456 UHPLC-MS/MS based target profiling of stress-induced phytohormones. *Phytochemistry* 105,
457 147–157. 10.1016/J.PHYTOCHEM.2014.05.015.
- 458 32. Zelm, E. van, Koevoets, I.T., Meyer, A.J., Velde, K. van der, Zeeuw, T.A.J. de, Verstappen, F.,
459 Holmer, R., Kohlen, W., Willemsen, V., Gommers, C.M.M., et al. (2023). CYP79B2 and CYP79B3
460 contribute to root branching through production of the auxin precursor indole-3-acetonitrile.
461 *bioRxiv*, 2023.09.26.559630. 10.1101/2023.09.26.559630.
- 462 33. Kurihara, D., Mizuta, Y., Sato, Y., and Higashiyama, T. (2015). ClearSee: A rapid optical clearing
463 reagent for whole-plant fluorescence imaging. *Development (Cambridge)* 142.
464 10.1242/dev.127613.
- 465
- 466
- 467
- 468